Title

Supramammillary regulation of locomotion and hippocampal activity.

Journal

The Scientific monthly, 374(6574)

Authors

Farrell, Jordan

Lovett-Barron, Matthew

Klein, Peter

et al.

Publication Date

2021-12-17

DOI

10.1126/science.abh4272

Peer reviewed

HHS Public Access

Author manuscript

Science. Author manuscript; available in PMC 2022 May 31.

Published in final edited form as:

Science. 2021 December 17; 374(6574): 1492–1496. doi:10.1126/science.abh4272.

Supramammillary regulation of locomotion and hippocampal activity

Jordan S. Farrell[1,*], **Matthew Lovett-Barron**[2,3], **Peter M. Klein**[1], **Fraser T. Sparks**[4,5,6], **Tilo Gschwind**[1], **Anna L. Ortiz**[1], **Biafra Ahanonu**[7,8], **Susanna Bradbury**[2], **Satoshi Terada**[4,5,6], **Mikko Oijala**[1], **Ernie Hwaun**[1], **Barna Dudok**[1], **Gergely Szabo**[1], **Mark J. Schnitzer**[7,9], **Karl Deisseroth**[2,9,10], **Attila Losonczy**[4,5,6], **Ivan Soltesz**[1]

[1]Department of Neurosurgery, Stanford University, Stanford, CA, USA

[2]Department of Bioengineering, Stanford University, Stanford, CA, USA

[3]Neurobiology Section, Division of Biological Sciences, University of California, San Diego, CA, USA

[4]Department of Neuroscience, Columbia University, New York, USA

[5]Kavli Institute for Brain Sciences, Columbia University, New York, USA

[6]Mortimer B. Zuckerman Mind Brain Behavior Institute, Columbia University, New York, USA

[7]Departments of Biology and Applied Physics, Stanford University, Stanford, CA, USA

[8]Department of Anatomy, University of California, San Francisco, CA, USA

[9]Howard Hughes Medical Institute, Stanford University, Stanford, CA, USA

[10]Department of Psychiatry and Behavioral Sciences, Stanford University, Stanford, CA, USA

Abstract

Locomotor speed is a basic input used to calculate one's position, but where this signal comes from is unclear. We identified neurons in the supramammillary nucleus (SuM) of the rodent hypothalamus that were highly correlated to future locomotor speed and reliably drove locomotion when activated. Robust locomotion control was specifically identified in Tac1 (substance P)-expressing neurons (SuM^{Tac1+}), whose activation selectively controlled the activity of speed-modulated hippocampal neurons. In contrast, SuM^{Tac1-} cells weakly regulated locomotion, but

*Corresponding author. jsfarrel@stanford.edu.

Author contributions:
Conceptualization: JSF, IS
Methodology: BA, MO, GS
Investigation: JSF ML-B, PMK, FTS, TG, AO, SB
Formal Analysis: JSF ML-B, PMK, FTS, TG, ST, MO, EH, BD
Funding acquisition: MJS, KD, AL, IS
Supervision: MJS, KD, AL, IS
Writing – original draft: JSF, IS
Writing – review & editing: All authors

Competing interests: M.J.S. is a scientific co-founder of Inscopix. GRIN lenses used in this studied were purchased from Inscopix

Data and materials availability: Code used in this manuscript came from publicly available resources referenced in the Material and Methods. Parts of the raw datasets and additional custom code are openly available at solteszlab.com/datasets and will continue to be formatted and uploaded.

potently controlled the spike-timing of hippocampal neurons and were sufficient to entrain local network oscillations. These findings highlight that the SuM not only regulates basic locomotor activity but also selectively shapes hippocampal neural activity in a manner that may support spatial navigation.

One-Sentence Summary:

Dissociated hypothalamic cell-types differentially drive locomotion and hippocampal cellular and network-level activity patterns.

Constructing and accessing a mental map of the environment during locomotion is an important adaptation facilitating survival and is supported by tracking self-motion (1). Mammalian locomotion is intimately tied to the occurrence of 6–12Hz hippocampal theta oscillations, such that theta begins prior to the onset of self-generated motion and increases in amplitude with respect to speed (*2–6*). Hippocampal theta temporally organizes the activity of place-coding neuronal assemblies into trajectories across past, present, and future locations, which is thought to subserve cognitive operations during spatial navigation (*5–10*). Tight coupling of theta to speed could be the result of shared neural circuitry between self-generated locomotion and theta control, providing a potential speed signal (1). Alternatively, speed could be derived from optic flow, vestibular input, or an efference copy from locomotor areas (*11–14*). Since the identification of speed-encoding neurons in brain areas like the hippocampus and entorhinal cortex that are thought to utilize a speed signal to calculate position (*3,15–18*), there is growing interest in understanding potential sources of speed input.

The medial septum is critical for hippocampal theta and is functionally coupled to locomotion (*3, 19–21*), but other brain areas have been proposed to contribute to this oscillation. One such area is the supramammillary nucleus (SuM) of the posterior hypothalamus (*22–24*), which also has recently identified roles in arousal (25), spike-timing coordination (26), and identification of novelty (27). As a proposed theta controller, neural activity in the SuM is likely also related to locomotion, but this has not been systematically investigated. In addition to innervating the medial septum, the SuM has highly divergent outputs targeting midbrain, where locomotor commands are integrated and brain regions involved in spatial navigation, including the hippocampus, entorhinal cortex, medial prefrontal cortex, nucleus reuniens, and claustrum (28). Thus, the SuM projects to theta, locomotor, and spatial navigation circuitry, but the functional relevance of this positioning remains poorly understood.

Using electrophysiological data from rats navigating a continuous alternation task for reward (26), we first investigated how the spiking activity of SuM neurons relates to locomotor speed and hippocampal theta oscillations (Fig. 1A). Similar to previous observations in the midbrain locomotor region (MLR) (29), we found a large proportion of SuM units with firing rates that were significantly coupled to locomotor speed with the majority displaying a positive correlation (Fig. 1B,C; fig. S1A,C,D). Interestingly, SuM “speed cells” were more correlated with future speed, with an average offset of 1.2 seconds, than real-time speed (Fig. 1D, fig S1A,D). After adjusting for temporal offsets, the firing rate of 99% of SuM

units were modulated by speed (fig. S1B). Most speed cells retained their correlation with immobility data withheld (fig. S1E,F) and were more weakly coupled to acceleration than speed (fig. S2). SuM unit activity was also correlated to hippocampal theta amplitude in real-time, but this was less accurately modeled than speed (fig. S3). Thus, SuM activity and locomotion are strongly coupled.

We then addressed whether speed-related neuronal activity is propagated to projection targets, because not all locally recorded SuM units are necessarily projection neurons. *In vivo* 2-photon calcium imaging of SuM axon terminals innervating the dentate gyrus (DG) and CA2 of hippocampus was performed on head-fixed mice (fig. S4A). Indeed, speed-correlated activity in SuM axons was observed in both regions (fig. S4B,C). Extensive collateralization of SuM axons was also determined (fig. S5) and may contribute to the similar proportion of positively and negatively correlated cells in both regions (fig. S4B).

Next, we examined the coupling between SuM action potentials and hippocampal theta waves (Fig. 1E). 30.7% of units displayed high coherence with hippocampal theta and theta-rhythmic spiking (Fig. 1F,G, see methods). SuM “theta cells” typically fired near the trough of CA1 theta with a slight prospective bias (fig. S6). Much like the overall SuM population, most SuM theta cells were positively correlated with locomotor speed (Fig. 1H).

To test the functional involvement of the SuM in locomotion and theta, we injected the SuM with recombinant adeno-associated virus (rAAV) to express the optogenetic proteins, channelrhodopsin-2 (ChR2, excitatory) or halorhodopsin (HR, inhibitory), under control of a pan-neuronal promoter (Fig. 2A,G). Light activation of ChR2 drove locomotion on 100% of trials with an average latency of 2.4±0.6 seconds in head-fixed mice (Fig. 2B–F). Locomotion lagged behind an increase in theta amplitude (fig. S7), which is consistent with prospective encoding of speed but real-time encoding of theta amplitude (Fig. 1D vs. fig. S3A). The frequency of laser pulses reliably entrained hippocampal local field potential (LFP) at 8 and 12 Hz (Fig. 2G,H), similar to previous optogenetic manipulations in the medial septum (*3,4,20,21*). 94% of CA1 neurons were entrained by laser pulses, however, the preferred firing phase shifted considerably from spontaneous theta (fig. S8). Optogenetic inhibition with HR halted locomotion on 65.6±0.6 % of trials with a latency of 5.4±0.2 seconds (Fig. 2B–F). Consistent with previous studies (*26,30*), SuM inhibition did not alter hippocampal theta during locomotion (Fig. 2G,H). Thus, optogenetic manipulation of the SuM robustly and bidirectionally controls locomotion but does not inhibit spontaneous hippocampal theta, despite robust spike and LFP entrainment with ChR2.

Considering the heterogeneity of SuM cell types (31), we then determined if locomotion control and spike/LFP entrainment were cell-type dependent. A subset of SuM neurons express Substance P, encoded by the Tac1 gene, and project to the hippocampus and other regions (32). Using the Tac1-Cre mouse line, we targeted two mutually exclusive populations. SuM^{Tac1+} neurons were labelled with a CreON rAAV, whereas a smaller population of SuM^{Tac1-} projection neurons were labelled with an intersectional approach using a CreOFF-FlpON rAAV (33), facilitated by a retrograde rAAV carrying Flp in the medial septum (Fig. 3A,B). The axon outputs of both cell populations were similar, innervating the known and expected SuM target regions (Fig. 3C; fig. S9). However,

SuM^{Tac1+} and SuM^{Tac1-} cells had different intrinsic properties (fig. S10). Cell-types were further differentiated by the non-uniform axon innervation pattern of the dentate gyrus granule cell layer (fig. S11C) and increased vesicular GABA transporter content of SuM^{Tac1-} cells (fig. S11A,B), consistent with previously identified GABA/glutamate co-releasing SuM cells (34). Functionally, SuM^{Tac1+} cell stimulation robustly drove locomotion on 100% of trials (Fig. 3D–G) but did not entrain hippocampal LFP (Fig. 3H). This locomotion was relatively slow and steady with an alternating stepping pattern (movie S1), consistent with exploratory locomotion and distinct from fight or flight responses seen with stimulation of other hypothalamic areas (35). In contrast, activation of SuM^{Tac1-} cells weakly controlled locomotion (Fig. 3D–G), but precisely controlled the frequency of hippocampal LFP at 8 and 12 Hz (Fig. 3H).

Given the robust control of movement initiation by SuM^{Tac1+} neuron stimulation, we further examined the role of this cell-type in locomotion. Using 2-photon calcium imaging in head-fixed behaving mice, we observed a high proportion of SuM^{Tac1+} cells whose activity were positively correlated with speed and active prior to locomotion onset (fig. S12). Similar results were obtained from Tac1+ cells in the ventral hypothalamus of zebrafish during swimming behavior, supporting evolutionary conservation of function (fig. S13). As with broad SuM inhibition, selective optogenetic inhibition of SuM^{Tac1+} neurons also suppressed locomotion in head-fixed mice (fig. S14). Finally, we examined potential SuM^{Tac1+} output pathways that reach the MLR, where the coordination of locomotor input and gait selection takes place (36). Using anterograde trans-synaptic tracing to label post-synaptic neurons (37), we found that midbrain periaqueductal grey neurons that specifically receive SuM^{Tac1+} input, in turn, project to the MLR (fig. S15).

Finally, we determined how SuM^{Tac1+} and SuM^{Tac1-} neurons alter firing rate and control the spike-timing of hippocampal neurons. Given the tight coupling of SuM^{Tac1+} cells to locomotion, we hypothesized that spontaneously speed-correlated hippocampal neurons would be particularly sensitive to SuM^{Tac1+} activation. On average, activation of both SuM cell-types increased the firing rate of the hippocampal units during locomotion (Fig. 4B) and resulted in similar proportions of units with significant firing rate alterations (Fig. 4A). The effect of SuM^{Tac1+}, but not SuM^{Tac1-} stimulation, was indeed correlated to the magnitude of spontaneous speed-modulation, such that the firing rates of positively correlated speed units increased, and negatively correlated cells decreased with optogenetic stimulation (Fig. 4B). We observed the opposite relationship with optogenetic inhibition of SuM^{Tac1+} cells (fig. S14E). Hippocampal speed cell firing rates were then modelled from speed and laser timing as inputs (Fig. 4C). Modeling firing rates during SuM^{Tac1+} stimulation produced considerably less error than SuM^{Tac1-} stimulation when laser timing was withheld (Fig. 4C), supporting that the effect of SuM^{Tac1+} stimulation on locomotion and hippocampal speed cell firing rates are coupled.

At a sub-second timescale, we also determined if hippocampal spike timing was altered relative to each laser pulse. Because SuM^{Tac1-} activation overrode spontaneous hippocampal theta and entrained LFP, we hypothesized that spike-timing would be more affected by activation of this cell-type. Indeed, SuM^{Tac1-} activation entrained spike-timing in more units with a greater average effect (Fig. 4D,E). Moreover, SuM^{Tac1-} activation increased

the firing rate of most units in close proximity to the termination of each light pulse, whereas SuM^{Tac1+} activation had mixed responses (Fig. 4F, fig. S16). Unlike SuM^{Tac1-} stimulation, the effect of SuM^{Tac1+} stimulation depended on that unit's speed correlation, such that positively correlated hippocampal speed cells were more likely to fire shortly after laser pulse onset and negatively correlated cells were suppressed (Fig. 4G). A significant correlation between the magnitude of optogenetic entrainment and the magnitude of spontaneous theta entrainment was observed for activation of both cell-types. In addition to the greater overall optogenetic entrainment (Fig. 4E), SuM^{Tac1-} activation resulted in a two-times greater slope of the optogenetic vs. spontaneous theta entrainment linear fit (Fig. 4H). Lastly, the preferred firing phase relative to hippocampal theta was more perturbed by SuM^{Tac1-} cell activation (fig. S17).

The finding that SuM^{Tac1-} cells potently regulate hippocampal spike-timing and are sufficient to entrain LFP is interesting in light of the lack of effect of SuM inhibition on spontaneous hippocampal theta. However, others have reported no change in hippocampal theta with SuM inhibition and lesions (*26,30*), despite remarkable effects with SuM activation (31). Recent work demonstrated that a sub-population of SuM units increase their activity under novel conditions (27). SuM cells from this previous study have several characteristics that overlap with SuM^{Tac1-} cells, including the non-uniform axonal innervation pattern and mixed neurotransmitter phenotype in the dentate gyrus (34). In another study, optogenetic inhibition of the SuM affected theta-range spike-timing in SuM-connected structures, but only at the decision point of the maze (26). Thus, SuM^{Tac1-} cells may be most influential to hippocampal network patterns in particularly salient situations, with little contribution to mechanisms underlying spontaneous theta. Consistent with this model, SuM^{Tac1-} activation caused a considerable shift in firing phase preferences from spontaneously generated theta, highlighting potentially different underlying mechanisms for SuM^{Tac1-}-evoked vs. spontaneous theta.

These data also advance our understanding of the SuM's in role in locomotion and identifies a cell-type with functional properties relevant to spatial navigation. In addition to the tight coupling of SuM^{Tac1+} activity to speed, we found that SuM^{Tac1+} activation robustly drove locomotion while selectively regulating the activity of speed-sensitive hippocampal neurons. These data raise the intriguing potential role for SuM^{Tac1+} neurons in distributing a speed signal throughout its many axon-termination sites and complements recent work outlining a pathway from the MLR to entorhinal cortex via the septum that relays speed (38). Given that SuM^{Tac1+} cells encode future speed, the SuM may provide its synaptic partners with intended speed whereas executed speed is propagated from the MLR. Thus, the SuM may support a role in planning and error correction during locomotion by broadcasting a future speed signal.

Supplementary Material

Refer to Web version on PubMed Central for supplementary material.

Acknowledgments:

The authors thank Hiroshi Ito, Edvard Moser, and May-Britt Moser for generously sharing a previously published dataset for reanalysis for the specific purposes of this study and providing comments on the manuscript. The authors also thank Rika Kumar and Sylwia Felong for technical assistance.

Funding:

Canadian Institutes of Health Research postdoctoral fellowship (JSF)

National Institute of Mental Health (NIMH) K99MH11284002 (MLB)

American Epilepsy Society (AES) Junior Investigator Award (FTS)

Stanford Epilepsy Training Grant funded by the National Institute of Neurological Disorders and Stroke (NINDS) 5T32NS007280 (PMK, EH)

Swiss National Science Foundation Postdoctoral Fellowship (TG)

National Science Foundation Fellowship DGE-114747 (BA)

HHMI Gilliam Fellowship for Advanced Study (BA)

Gates Millennium Scholarship (BA)

Japan Society for the Promotion of Science (JSPS) Overseas (ST) Fellowship.

AES Postdoctoral Fellowship (BD)

NINDS K99NS117795 (BD)

National Institute of Health (NIH) 1U19NS104590 (IS, AL, MS).

NIMH 1R01MH124047 and 1R01MH124867 (AL)

Kavli Foundation (AL)

NIH, NSF, Gatsby, Fresenius, and NOMIS Foundations (KD).

References and Notes

1. O'Keefe J, Nadel L, The hippocampus as a cognitive map (Oxford: Clarendon Press, 1978).
2. Vanderwolf CH, Electroencephalogr. Clin. Neurophysiol. 26, 407–418 (1969). [PubMed: 4183562]
3. Foster TC, Castro CA, McNaughton BL, Science 244, 1580–1582 (1989). [PubMed: 2740902]
4. Fuhrmann F, et al. Neuron, 86, 1253–1264 (2015). [PubMed: 25982367]
5. Colgin LL, Mechanisms and functions of theta rhythms. Annu. Rev. Neurosci. 36, 295–312 (2013). [PubMed: 23724998]
6. Buzsáki G. Rhythms of the Brain (Oxford University Press, 2006).
7. O'Keefe J, Recce ML, Hippocampus 3, 317–330 (1993). [PubMed: 8353611]
8. Skaggs WE, McNaughton BL, Wilson MA, Barnes CA, Hippocampus 6, 149–172 (1996). [PubMed: 8797016]
9. Pastalkova E, Itskov V, Amarasingham. A, Buzsáki G, Science 321, 1322–1327 (2008). [PubMed: 18772431]
10. Mehta MR, Lee AK, Wilson MA, Nature 417, 741–746 (2002). [PubMed: 12066185]
11. Sheeran WM, Ahmed OJ, Neurosci. Biobehav. Rev. 108, 821–833 (2020). [PubMed: 31760048]
12. Munn RG, Mallory CS, Hardcastle K, Chetkovich DM, Giocomo LM, Nat. Neurosci. 23, 239–251 (2020). [PubMed: 31932764]
13. Perez-Escobar JA, Kornienko O, Latuske P, Kohler L, Allen K, K. eLife 23, e16937 (2016).

14. Campbell MG et al. Nat. Neurosci. 21, 1096–1106 (2018). [PubMed: 30038279]
15. Iwase M, Kitanishi T, Mizuseki K, Sci. Rep. 10, 1–23 (2020). [PubMed: 31913322]
16. Kropff E, Carmichael JE, Moser MB, Moser EI, Nature 523, 419–424 (2015). [PubMed: 26176924]
17. Justus D, et al. Nat. Neurosci. 20, 16–19 (2017). [PubMed: 27893726]
18. Hinman JR, Brandon MP, Climer JR, Chapman GW, Hasselmo ME, Neuron 91, 666–679 (2016). [PubMed: 27427460]
19. Green JD, Arduini AA, J. Neurophysiol 17, 533–557 (1954). [PubMed: 13212425]
20. Dannenberg H, et al. J. Neurosci. 35, 8394–8410 (2015). [PubMed: 26041909]
21. Zutshi I, et al. Current Biology 28, 1179–1188 (2018). [PubMed: 29628373]
22. Kirk IJ, McNaughton N, Neuroreport 2, 723–725 (1991). [PubMed: 1810464]
23. Kirk IJ, Oddie SD, Konopacki J, Bland BH, J. Neurosci 16, 5547–5554 (1996). [PubMed: 8757266]
24. Kocsis B, Vertes RP, J. Neurosci 14, 7040–7052 (1994). [PubMed: 7965097]
25. Pedersen NP, et al. Nat. Comm. 8, 1–16 (2017).
26. Ito HT, Moser EI, Moser MB, Neuron 99, 576–587 (2018). [PubMed: 30092214]
27. Chen S, et al. Nature 586, 270–274 (2020). [PubMed: 32999460]
28. Vertes RP, J. Comp. Neurol. 326, 595–622 (1992). [PubMed: 1484125]
29. Lee AM, et al. Neuron 83, 455–466 (2014). [PubMed: 25033185]
30. Thinschmidt JS, Kinney GG, Kocsis B, Neuroscience 67, 301–312 (1995). [PubMed: 7675171]
31. Pan WX, McNaughton N, Prog. Neurobiol. 74:127–66 (2004). [PubMed: 15556285]
32. Ino T, et al. Neurosci. Lett. 90, 259–264 (1988). [PubMed: 2458555]
33. Fenno LE, et al. Nat. Methods 11, 763–772 (2014). [PubMed: 24908100]
34. Billwiller F, et al. Brain Struct. Funct 225, 1–26 (2020). [PubMed: 31792694]
35. Li Y, et al. Neuron 97, 911–924 (2018). [PubMed: 29398361]
36. Caggiano V, et al. Nature 553, 455–460 (2018). [PubMed: 29342142]
37. Zingg B, et al. Neuron 93, 33–47 (2017). [PubMed: 27989459]
38. Carvalho MM, et al. Cell Rep. 32, 108123 (2020). [PubMed: 32905779]
39. Harris JA et al. Front. Neural Circuits 8, 76 (2014). [PubMed: 25071457]
40. Kropff E, Carmichael JE, Moser MB, Moser EI, Neuron 109, 1–11 (2021). [PubMed: 33412092]
41. Fries P, Reynolds JH, Rorie AE, Desimone R, Science 291, 1560–1563 (2001). [PubMed: 11222864]
42. Rutishauser U, Ross IB, Mamelak AN, Schuman EM, Nature 464, 903–907 (2010). [PubMed: 20336071]
43. Siapas AG, Lubenov EV, Wilson MA, Neuron 46,141–51 (2005). [PubMed: 15820700]
44. Dana H, Nature Methods 16, 649–657 (2019). [PubMed: 31209382]
45. Chen TW, Nature 499, 295–300 (2013). [PubMed: 23868258]
46. Mahn M, et al. Nat. Comm. 9, 1–15 (2018).
47. Madisen L et al. Neuron 85, 942–958 (2015). [PubMed: 25741722]
48. Kaifosh P, Lovett-Barron M, Turi GF, Reardon TR, Losonczy A, Nat. Neurosci. 16, 1182–1184 (2013). [PubMed: 23912949]
49. Danielson NB, et al. Neuron 90, 101–112 (2016). [PubMed: 26971949]
50. Sparks FT, Liao A, Li W, Grosmark A, Soltesz I, Losonczy A, A. Nat. Comm. 11, 1–13 (2020).
51. Chung JE, Neuron 95, 1381–1394 (2017). [PubMed: 28910621]
52. Ting JT, Daigle TL, Chen Q, Feng G, G. “Acute brain slice methods for adult and aging animals: application oftargeted patch clamp analysis and optogenetics” in Patch-Clamp Methods and Protocols, Martina M, Taverna S, Eds (Springer New York, ed. 2, 2014).
53. Kaifosh P, Zaremba JD, Danielson NB, Losonczy A, Front. Neuroinform. 8, 80 (2014). [PubMed: 25295002]
54. Pachitariu M, et al. 10.1101/061507v2 (2017).

55. Freeman J, et al. Nat. Methods 11, 941–950 (2014). [PubMed: 25068736]
56. Štih V, Petrucco L, Kist AM, Portugues R, PLoS Comput. Biol. 15, e1006699 (2019). [PubMed: 30958870]
57. Lovett-Barron M, et al. Nat. Neurosci. 23, 959–967 (2020). [PubMed: 32572237]
58. Lovett-Barron M et al. Cell, 171: 1411–1423 (2017). [PubMed: 29103613]
59. H. M. Choi, et al. Development 145, dev165753 (2018). [PubMed: 29945988]
60. Harris CR, et al. Nature 585, 357–362 (2020). [PubMed: 32939066]
61. Hunter JD, Comput. Sci. Eng. 9, 90–95 (2007).
62. Virtanen P, et al. Nat. Methods 17, 261–272 (2020). [PubMed: 32015543]
63. Pedregosa F, J. Mach. Learn. Res. 12, 2825–2830 (2011).
64. Robitaille TP et al. Astron. Astrophys. 558, A33 (2013).
65. Berens P, J. Stat. Softw. 31, 1–21 (2009).

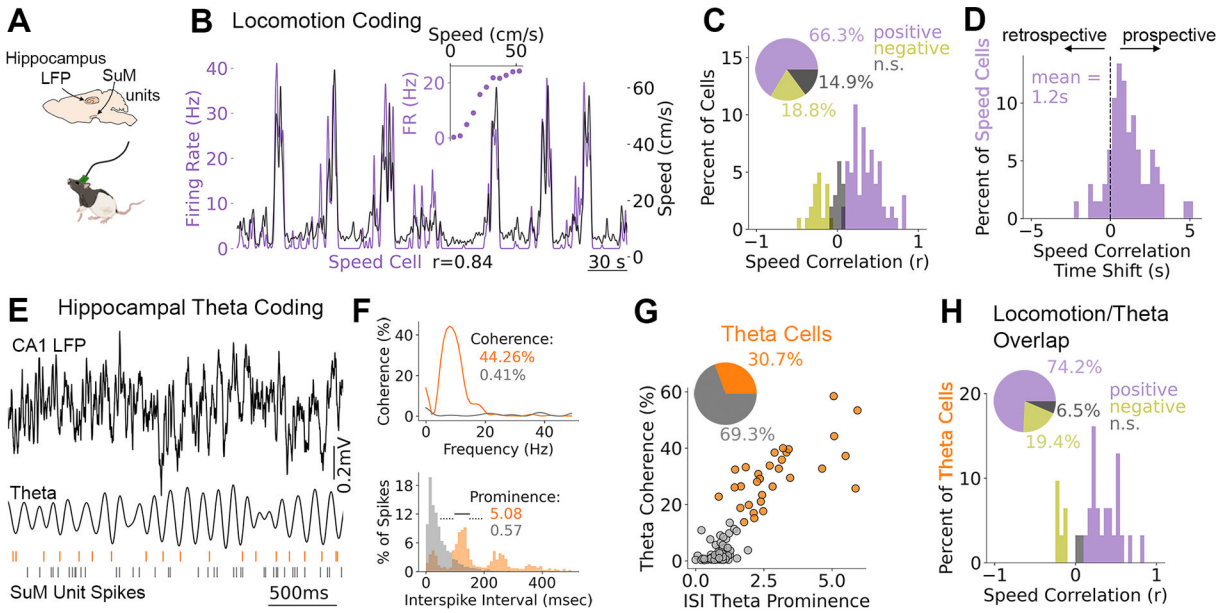

Fig. 1. SuM representation of speed and hippocampal theta

A, Recording paradigm; data from using unrestrained rats (26), reanalyzed here for speed- and theta-related investigations. **B**, Example SuM unit (recorded by tetrodes) that positively correlates to speed (i.e. a speed cell). Inset represents these data as a scatter plot. **C**, Distribution of speed vs. firing rate Pearson r values. Pie chart shows percentage of units for positive (r=0.36±0.023, mean±sem), negative (r=−0.24±0.024), and non-significant cells (r=0.018±0.012). **D**, Distribution of temporal offsets for positive speed cells. sem=0.19. **E**, Two example SuM unit spiking activities. Orange cell shows phase-locked firing with respect to hippocampal theta whereas the grey cell does not. **F**, Quantification of theta-related firing for two example units from *E*. The top panel shows spike-field coherence and the bottom shows theta-rhythmic spiking. **G**, Units were clustered into theta cells based on quantification from *F*. **H**, Distribution of speed scores among clustered “theta cells” from *G*.

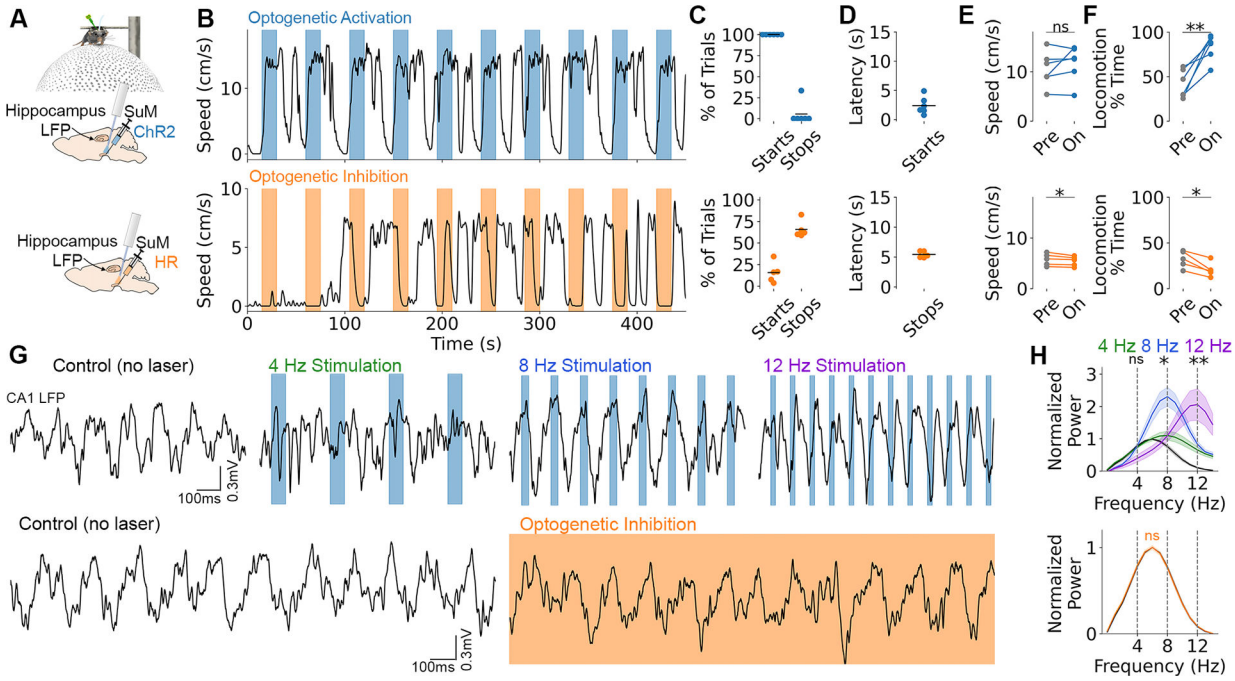

Fig. 2. Optogenetic SuM modulation controls locomotion and hippocampal LFP

A, Pan-neuronal SuM activation with ChR2 (blue) or inhibition with HR (orange) in head-fixed mice on a floating ball. **B**, Bidirectional locomotor effect with SuM activation (top) and inhibition (bottom). Colored bars denote laser on. **C**, Percent of trials where locomotion was initiated or halted for ChR2 (top) and HR (bottom). **D**, Latency of start vs. stop response. **E**, Speed during locomotor epochs before (pre) and during (on) light delivery. ChR2, t_5=−1.14, p=0.31; HR, t_4=3.07, p=0.037. **F**, Percent of time spent locomoting before (pre) and during (on) light delivery. ChR2, t_5=−4.84, p=0.0047; HR, t_4=4.60, p=0.010. **G**, Top: optogenetic activation at 4, 8, or 12Hz compared to no laser control. Blue bars denote laser on. Bottom: optogenetic inhibition (orange shading) vs. no laser control. Scalebar applies across rows. **H**, Quantification of power spectrum changes normalized to no laser. Top (ChR2): 4Hz power at 4Hz stimulation, t_5=0.86, p=0.43; 8Hz power at 8Hz stimulation, t_5=5.18, p=0.0035; 12Hz power at 12Hz stimulation, t_5=3.99, p=0.010. Bottom (HR): t_4=0.043, p=0.97. Data are mean±sem.

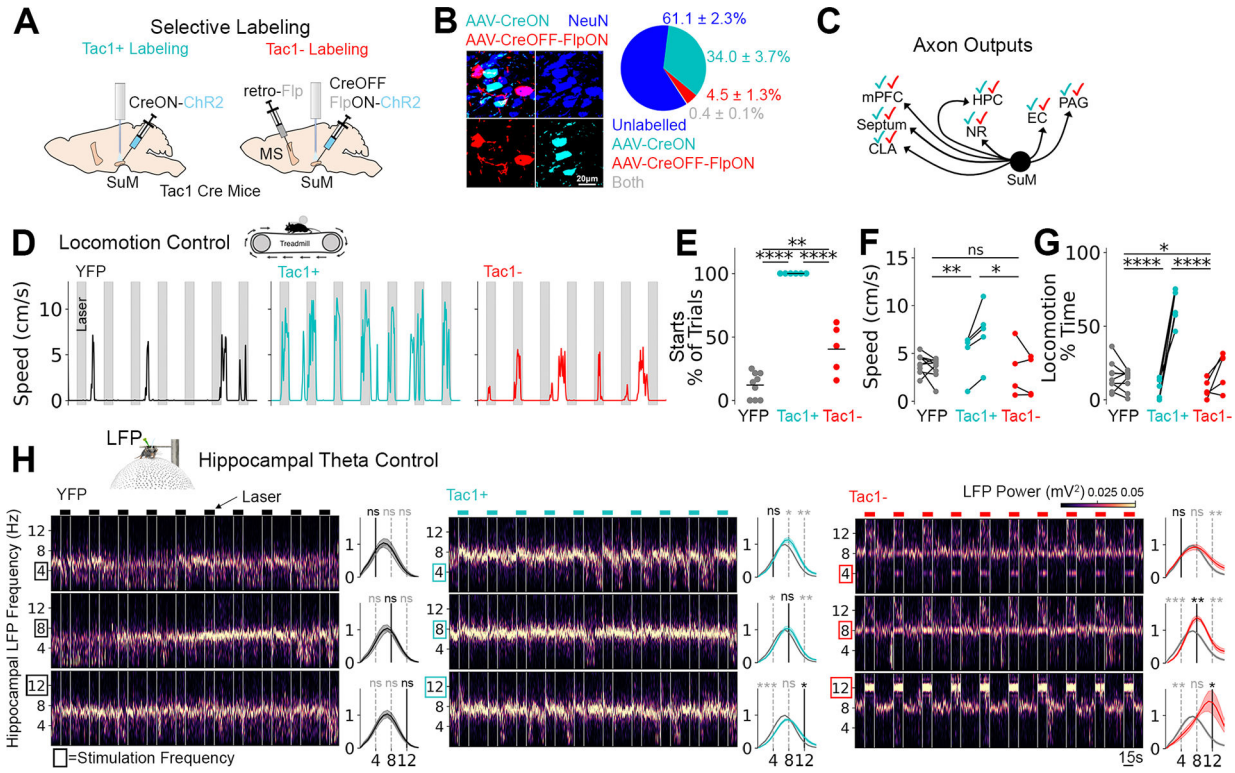

Fig. 3. Cell-type-dependence of locomotion initiation and LFP entrainment

A, Labeling strategy to target mutually exclusive populations based on Tac1. **B**, Investigation of labelling specificity. Left: Image showing AAV-labelled Tac1+ (CreON) and Tac1− cells (CreOFF-FlpON) among other NeuN+ cells in the SuM. Right: quantification. **C**, Schematic showing checkmarks of each color (cyan: SuM^{Tac1+}, red: SuM^{Tac1-}) if axons were found in SuM target regions (see fig. S9). **D**, Representative locomotor activity during optogenetic activation at 8Hz. **E**, Percent of trials with locomotion initiation. ANOVA $F_{2,17}$=103.6, p<0.0001, Tukey post-test. **F**, Locomotor speed before (left) vs. laser on (right). ANOVA was performed to determine group differences on changes in speed (pre vs. on). $F_{2,15}$=7.2, p=0.0064, Tukey post-test. **G**, Percent of time locomoting before (left) vs. laser on (right). Differences in response change was assessed by ANOVA $F_{2,17}$=57.8, p<0.0001, Tukey post-test. **H**, Optogenetic stimulation while head-fixed on floating ball at 4, 8, or 12 Hz. Spectrogram (left) and power spectral density changes (right, off vs. on) for each condition (columns) at each frequency (rows). Paired t-tests performed on light off vs. light on. *p<0.05, **p<0.01, ***p<0.001, ****p<0.0001.

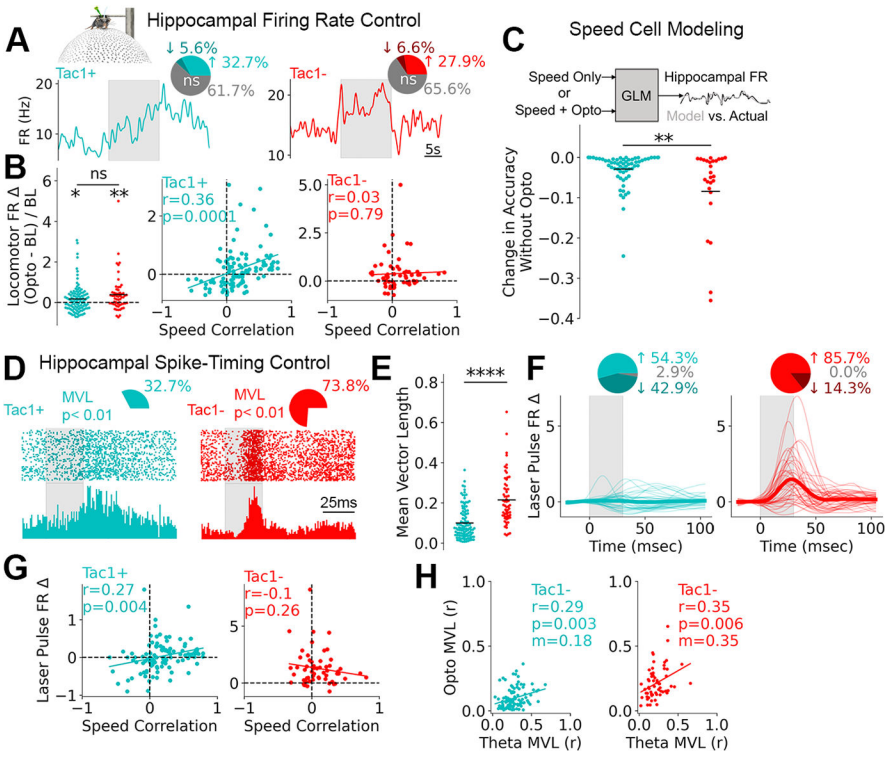

Fig. 4. Hippocampal populations are differentially regulated by SuM cell-types

A, Data were obtained from head-fixed mice on floating ball. Mean firing rate changes from two example hippocampal cells during SuM^{Tac1+} or SuM^{Tac1-} optogenetic activation (grey bar). Pie charts display proportion of units with significantly altered locomotor firing rates. **B**, Locomotor firing rate change for light on vs. off (one-sample t-test, SuM^{Tac1+} t_{105}=2.56, p=0.012; SuM^{Tac1-} t_{57}=3.28, p=0.0017; between sample t-test, t_{163}=1.69, p=0.09) and as a function of speed correlation (calculated while laser is off). Y-label applies to all panels. **C**, Generalized linear model of hippocampal speed cell FR, with two sets of input (speed only vs. speed + opto). Change in modelling accuracy when optogenetic information was withheld (t_{89}=3.28, p=0.0015). **D**, Hippocampal spike raster plots with histogram aligned to laser pulses (grey bar) during 8Hz stimulation. Pie charts show the proportion of units with significantly laser-modulated spike distributions. **E**, Quantification of non-uniform spike distributions from D. t-test t_{167}=7.39, p=6.8×10^{12}. **F**, Smoothed spike histograms of significantly laser-modulated cells. Thin lines are individual cells. Thick line is mean. Pie chart shows the directionality of modulation. **G**, Laser pulse-triggered firing rate change plotted against cells' speed correlations (calculated while laser is off). **H**, Firing rate modulation by spontaneous theta vs. optogenetic laser pulses. Lines in B, G and H represent linear fits.